PRAMANA
journal of
physics

© Printed in India

Supplement to Vol. 45
October 1995
pp. 277-292

Structure functions and parton distributions

R G ROBERTS
Rutherford Appleton Laboratory, Chilton,
Didcot OX11 0QX, England

Abstract. We review recent developments in the determination of parton densities from deep inelastic and related data. We show how the asymmetries observed in the $W^{\pm}$ rapidity distributions and in pp/pn Drell-Yan production further constrain the partons at moderate x.

1. Introduction

An idea of the rapid improvement in our knowledge of the structure function, $F_2(x, Q^2)$, of deep inelastic electron (or muon)-proton scattering can be glimpsed from the data shown in Fig. 1. In fact it should not be too long before we have precision measurements (perhaps as good as $\pm 5\%$) of F_2 at HERA almost down to $x \sim 10^{-4}$. The data show a dramatic rise of F_2 with decreasing x, which some optimists had anticipated might occur from the precocious onset of the leading $\alpha_s \log(1/x)$ resummation of soft gluon emissions.

The curves marked D'_- and D'_0 are simply two extrapolations obtained from parton fits to the fixed target data, which at the time it was thought might span the subsequent measurements of F_2 at HERA – one represents the upper limit expected for the precocious resummation behaviour, the other the lower limit of conventional (Regge-motivated) expectations. Such extrapolations are notoriously unreliable.

Section 2 is mainly devoted to recent developments in the determination of partons in the $x \gtrsim 10^{-2}$ region. For the purposes of illustration we mainly concentrate on the MRS analyses. In Section 3 we discuss the description of F_2^{ep} at small x and find that both GLAP-based extrapolations and BFKL-based predictions have sufficient freedom to describe the HERA data.

2. Recent developments in the determination of parton densities

There is a long history of determining parton distributions from deep inelastic scattering and related data. The increased precision in the experimental measurements over the last couple of years has led to a considerable improvement in our knowledge of the partons, at least for $x \gtrsim 0.01$. The recent experiments are listed in Table 1, together with the leading order partonic subprocess, which help us to see which partons are constrained by the various processes. In particular it is useful to note

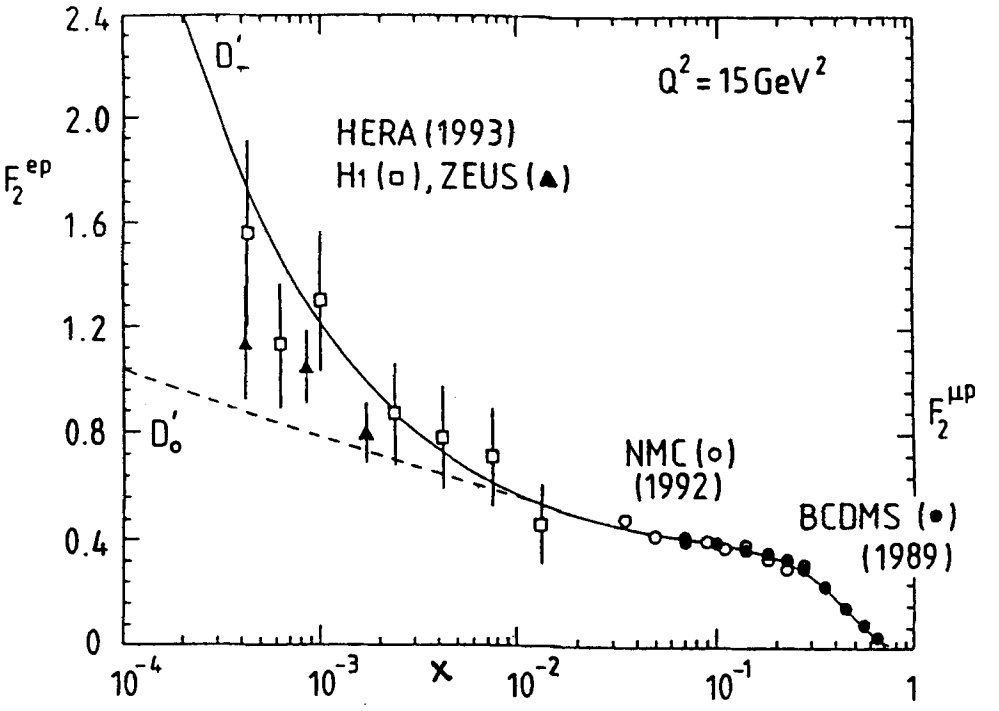

Figure 1. The x dependence of the structure function $F_2(x, Q^2)$ at $Q^2 = 15$ GeV^2. The data are from the BCDMS [1], NMC [2], H1 [3] and ZEUS [4] collaborations. The curves are calculated from the MRS(D'_0,D'_-) sets of partons [5].

that the four deep-inelastic structure functions can, to leading order, be expressed in terms of parton densities in the form

$$F_2^{\mu p} - F_2^{\mu n} = \tfrac{1}{3}x(u + \bar{u} - d - \bar{d}) \quad (1)$$

$$\tfrac{1}{2}(F_2^{\mu p} + F_2^{\mu n}) = \tfrac{5}{18}x(u + \bar{u} + d + \bar{d} + \tfrac{4}{5}s) \quad (2)$$

$$F_2^{\nu N} = F_2^{\bar{\nu} N} = x(u + \bar{u} + d + \bar{d} + 2s) \quad (3)$$

$$\tfrac{1}{2}x(F_3^{\nu N} + F_3^{\bar{\nu} N}) = x(u - \bar{u} + d - \bar{d}) \quad (4)$$

where N is an isoscalar nuclear target. We have included the s quark (and assumed [5] that $s = \bar{s}$), but neglected the small c quark contribution. These four observables, $F_i(x, Q^2)$, measured in the fixed-target ($\mu N \to \mu X$ and $\nu N \to \mu X$) deep-inelastic experiments, do not on their own determine the five distributions $u, d, \bar{u}, \bar{d}$ and s, but only four combinations, which we may take to be $u + \bar{u}$, $d + \bar{d}$, $\bar{u} + \bar{d}$ and s. The difference $\bar{d} - \bar{u}$ is not determined, and, moreover, at leading order it appears that the only constraint on the gluon is through the momentum sum rule. In practice the situation is worse. From (2) and (3) we see that the strange quark distribution is essentially determined by the structure function difference

$$xs(x) \simeq \tfrac{5}{6}F_2^{\nu N}(x) - 3F_2^{\mu D}(x) \quad (5)$$

which is sensitive to the relative normalization of the two data sets and to heavy target corrections to the neutrino measurements. However, we see from Table 1 that valuable independent information comes from other processes: (i) the gluon is constrained by prompt photon production, where $g(x)$ enters to leading order, (ii)

the strange sea is measured by neutrino-induced dimuon production (see Fig. 2), and (iii) there is a measurement of the difference $\bar{d} - \bar{u}$, which was released for the first time at this conference, from the observed asymmetry of Drell-Yan production in pp and pn collisions (see subsection (c)).

(a) MRS global analysis

Here we describe the MRS determination [6] of the parton densities, $f_i(x, Q^2)$, from a global analysis of the data, which was performed before the HERA measurements of F_2^{ep} became available. Only deep inelastic data with $Q^2 > 5$ GeV^2 (and $W^2 > 10$ GeV^2) were used. The input distributions at $Q_0^2 = 4$ GeV^2 were parametrized in the form

$$xf_i(x, Q_0^2) = A_i x^{-\lambda_i}(1-x)^{\beta_i}(1 + \gamma_i x^{\frac{1}{2}} + \delta_i x) \tag{6}$$

for $i =$ the valence quarks u_v, d_v, the sea S, and the gluon g. Three of the four A_i's are determined by the momentum and flavour sum rules. Since, pre-HERA, there were no data for $x < 10^{-2}$, we imposed two different extrapolations of the gluon and sea quark distributions to small x (with the expectation that they should span the forthcoming HERA measurements). To be precise for the gluon and sea quarks we choose

$$\begin{aligned} \lambda_i &\equiv 0 \quad \text{for the } D_0' \text{ set} \\ \lambda_i &\equiv 0.5 \quad \text{for the } D_-' \text{ set} \end{aligned} \tag{7}$$

where, since $\sigma(\gamma^* p) \sim s^{\lambda_i}$, the first choice corresponds to conventional Pomeron exchange leading to constant total cross sections, and the second is motivated by the small x behaviour expected from the BFKL (Balitsky, Fadin, Kuraev, Lipatov) equation [7]. The β_i and the valence λ_i are left as free parameters although we have some idea what values will be physically reasonable. First, the small x behaviour anticipated from meson Regge exchanges for the valence quark distributions would correspond to $\lambda_v \sim -0.5$. Secondly, naive counting rule arguments imply that $xf_i \sim (1-x)^{2n-1}$ as $x \to 1$, where n is the minimum number of spectator quarks which accompany the struck parton. This rule would suggest $\beta_i \sim 5$, 3 and 7 for, respectively, the gluon, valence and sea quark distributions.

In the MRS analysis the flavour structure of the quark sea S at $Q_0^2 = 4$ GeV^2 is taken to be

$$\begin{aligned} 2\bar{u} &= 0.4S - \Delta \\ 2\bar{d} &= 0.4S + \Delta \\ 2\bar{s} &= 0.2S \\ x\Delta &\equiv x(\bar{d} - \bar{u}) = A_\Delta x^{-\lambda_\Delta}(1-x)^{\eta_S}. \end{aligned} \tag{8}$$

As mentioned before, the most reliable method to estimate the strength of the strange sea distribution $\bar{s}(x, Q^2)$ is to observe deep-inelastic dimuon production, $\nu N \to \mu^- \mu^+ X$, for which the dominant subprocess is $\nu s \to \mu^- + c(\to \mu^+)$. Early dimuon data were the motivation of the 50% suppression of the input strange sea in the MRS analyses, which was assumed to be independent of x. Recently this input assumption has been checked by a next-to-leading order analysis performed by the CCFR collaboration [8] on their dimuon data. The MRS assumption is in

Table 1 The experimental data used to determine the MRS parton distributions. The last column gives an indication of the main type of constraint imposed by a particular set of data.

Process/ Experiment	Leading order subprocess	Parton determination
DIS $(\mu N \to \mu X)$ BCDMS, NMC $F_2^{\mu p}, F_2^{\mu n}$	$\gamma^* q \to q$	Four structure functions → $u+\bar{u}$, $d+\bar{d}$, $\bar{u}+\bar{d}$, s (assumed $=\bar{s}$), but only $\int xg(x)dx \simeq 0.5$ [$\bar{u}-\bar{d}$ is not determined]
DIS $(\nu N \to \mu X)$ CCFR (CDHSW) $F_2^{\nu N}, xF_3^{\nu N}$	$W^* q \to q'$	
$\nu N \to \mu^+\mu^- X$ CCFR	$\nu s \to \mu^- c \hookrightarrow \mu^+$	$s \approx \frac{1}{2}\bar{u}$ (or $\frac{1}{2}\bar{d}$)
DIS (HERA) F_2^{ep} (H1,ZEUS)	$\gamma^* q \to q$	λ $(x\bar{q} \sim xg \sim x^{-\lambda}$, via $g \to q\bar{q})$
$pp \to \gamma X$ WA70 (UA6)	$qg \to \gamma q$	$g(x \approx 0.4)$
$pN \to \mu^+\mu^- X$ E605	$q\bar{q} \to \gamma^*$	$\bar{q} = ...(1-x)^{\eta s}$
$pp, pn \to \mu^+\mu^- X$ NA51	$u\bar{u}, d\bar{d} \to \gamma^*$ $u\bar{d}, d\bar{u} \to \gamma^*$	$(\bar{u}-\bar{d})$ at $x = 0.18$
$pp \to WX(ZX)$ UA2, CDF, D0	$ud \to W$	u, d at $x_1 x_2 s \simeq M_W^2 \to$ $x \approx 0.13$ CERN, $x \approx 0.05$ FNAL
$\to W^{\pm}$ asym CDF		slope of u/d at $x \approx 0.05$

excellent agreement with their results (see Fig. 2) and moreover CCFR find that the ratio $\bar{s}/(\bar{u}+\bar{d})$ is essentially independent of x. It has been emphasized [9] that the strange sea as measured in neutrino scattering should be different from that in muon scattering on account of the different mass thresholds in $W^*g \to s\bar{c}$ versus $\gamma^*g \to s\bar{s}$. In practice the neutrino data have been corrected by CCFR to approximately take into account the $m_c \neq 0$ effects and allow for this difference.

The first evidence that $\bar{d} \neq \bar{u}$, and hence the need to introduce Δ in (8), came from the NMC study of the Gottfried sum rule [10]. We return to discuss this later. Finally, the heavy quark contributions are determined by assuming that

$$\bar{Q} = 0 \quad \text{for} \quad Q^2 \leq 4m_Q^2 \qquad \text{with} \quad Q = c, b, \ldots, \tag{9}$$

and by generating non-zero distributions at higher Q^2, via $g \to Q\bar{Q}$, using QCD evolution with $m_Q = 0$. Near threshold clearly this prescription is unreliable, but it has been shown to give reasonable results at higher Q^2 [11]. The charm quark distribution in the proton has attracted much attention but the phenomenological situation is far from clear.

The input distributions (6) and (8) are evolved up in Q^2 using next-to-leading order GLAP or Altarelli-Parisi equations [13] and fitted to deep-inelastic structure functions (with $Q^2 > 5$ GeV^2 and $W^2 > 10$ GeV^2) and related data. The distributions are defined in the $\overline{\text{MS}}$ renormalization and mass factorization scheme. The fitted value of the QCD scale parameter is $\Lambda_{\overline{\text{MS}}}(n_f = 4) = 230$ MeV (that is $\alpha_s(M_Z^2) = 0.112_5$), which is consistent with the values $\alpha_s = 0.113$ and 0.111 found by analyses of BCDMS [14] and CCFR [15] subsets of the overall data.

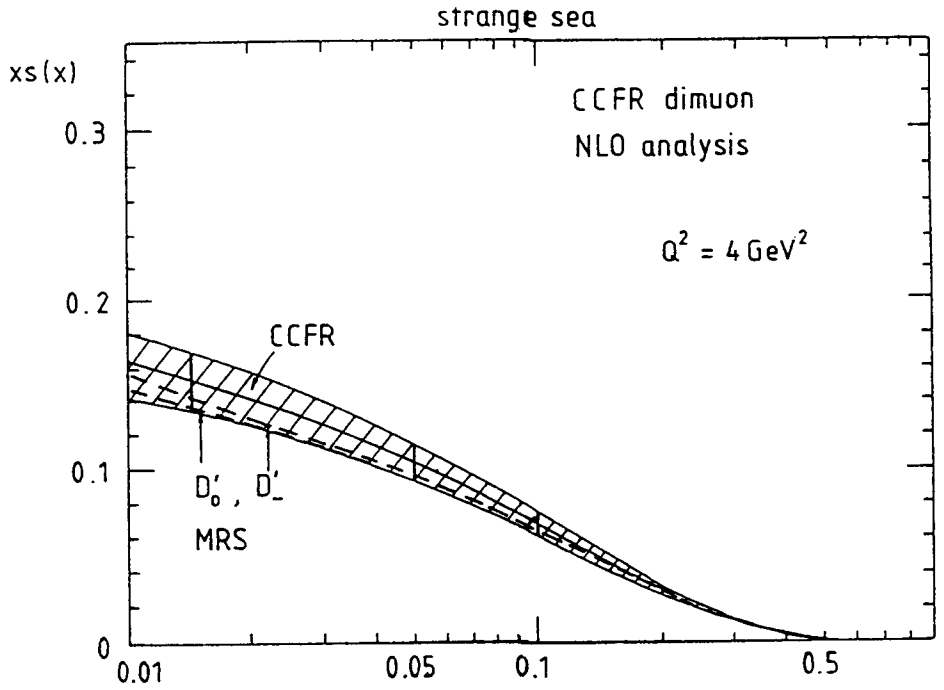

Figure 2. The shaded band shows the strange quark distribution extracted by CCFR from their dimuon data [7], together with the MRS distributions of ref. [5].

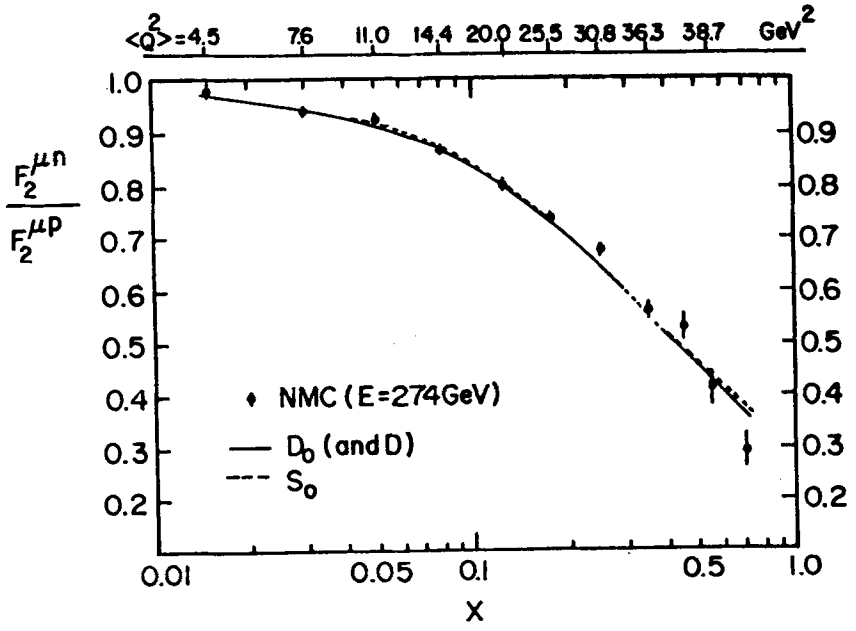

Figure 3. The description of the NMC data [2] for the structure function ratio $F_2^{\mu n}/F_2^{\mu p}$ given by the MRS partons of ref. [5].

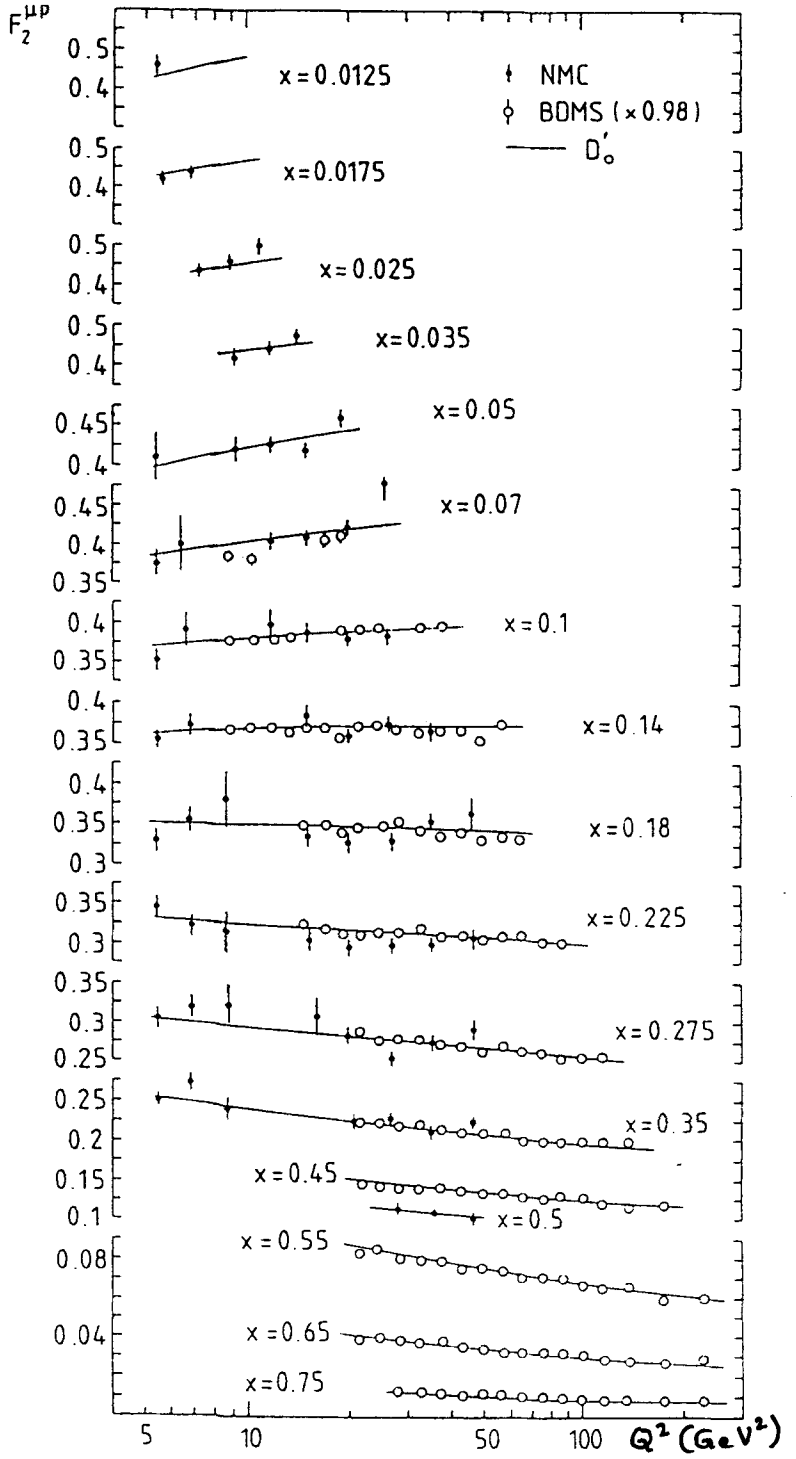

Figure 4. The BCDMS [1] and NMC [2] measurements of $F_2^{\mu p}$, together with the MRS fit [5].

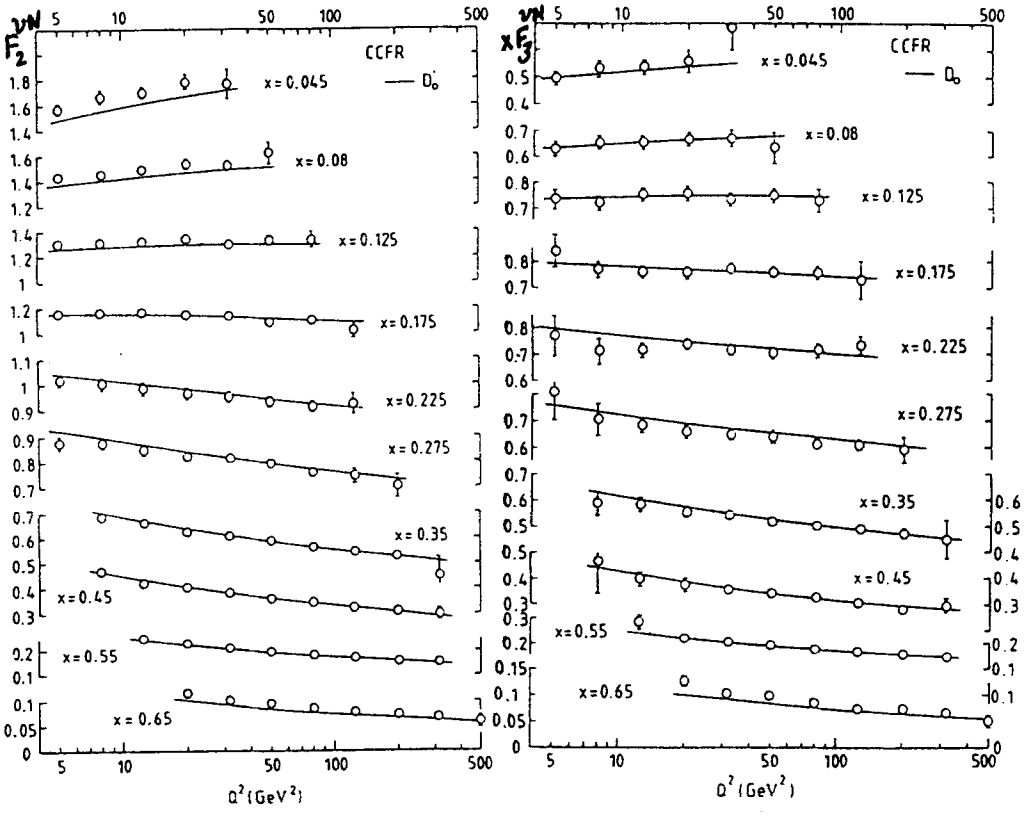

Figure 5. The continuous curves show the description of the CCFR [14] measurements of $F_2^{\nu N}(x, Q^2)$ and $xF_3^{\nu N}(x, Q^2)$ by the MRS(D_0') set of partons [5]. The data are shown after correction for the heavy target effects and after the overall renormalization of 0.95 required by the global fit.

Figs. 3-5 show the high precision of recent deep-inelastic structure function measurements, as well as the quality of the fit. Accurate data exist also for related processes and are equally well described. This should mean that the parton distributions are well determined, at least in the x range $0.02 \lesssim x \lesssim 0.7$ where data are available for a full range of different processes. At smaller x, $x \lesssim 10^{-3}$, the measurements of F_2^{ep} at HERA give information on the x behaviour of the quark sea. We will discuss the expectations of the small x behaviour in some detail later. For the moment we simply note that it is possible to 'tune' the exponent λ_i of the input sea and gluon distributions of (6) to obtain the best global fit to a data set which now includes the new HERA measurements of F_2 [3, 4]. The result, set MRS(H) of partons [16], has $\lambda_i = 0.3$.

Before turning to a theoretical discussion of the small x region, we must mention two recent measurements which impose valuable new constraints on the partons in the $x \gtrsim 0.02$ region. The first is the measurement of the rapidity asymmetry of $W^{\pm}$ bosons produced in $p\bar{p}$ collisions and the second is the Drell-Yan asymmetry observed in pp and pn collisions.

(b) $W^{\pm}$ rapidity asymmetry

$W^{\pm}$ bosons produced in $\bar{p}p$ collisions have different rapidity (y_W) distributions. A comparison of parton distributions shows that the u quark in the proton tends to go more forward than the d quark, so that the W^+ is produced preferentially in the direction of the incident proton, while the W^- tends to go in the direction of the antiproton. Thus we anticipate that the asymmetry

$$A_W(y_W) = \frac{\sigma(W^+) - \sigma(W^-)}{\sigma(W^+) + \sigma(W^-)} \tag{10}$$

will be positive and increase with the rapidity y_W of the produced $W^{\pm}$ bosons. It turns out that the asymmetry A_W is correlated with the slope of F_2^n/F_2^p in the $x \simeq M_W^2/\sqrt{s}$ region [17] – larger slopes tend to imply greater asymmetry. In practice it is the rapidity asymmetry of the $\ell^{\pm}$ decay leptons which is observed

$$A(y_\ell) = \frac{\sigma(\ell^+) - \sigma(\ell^-)}{\sigma(\ell^+) + \sigma(\ell^-)}. \tag{11}$$

Folding in the $W \to \ell\nu$ decay dilutes the asymmetry, but the measurements shown in Fig. 6 indicate that it is still sizeable. The present data favour the recent MRS rather than the CTEQ parton sets. As the experimental precision increases we see that there is a great potential for the asymmetry to further discriminate between parton sets – indeed these data should be included in future global analyses from the beginning.

(c) $\bar{d} - \bar{u}$ and the Drell-Yan asymmetry

Inspection of the leading order expressions (1)-(4) shows that measurement of the four independent deep-inelastic structure functions do not determine $\bar{d} - \bar{u}$ on a (x, Q^2) point-by-point basis. The difference $\bar{d} - \bar{u}$ is only constrained if the form of the x dependence of partons is assumed. Indeed prior to 1992 all global analyses set $\bar{u} = \bar{d}$. The first hint that $\bar{u} \neq \bar{d}$ came from an NMC study [21] of the Gottfried

sum rule. NMC found that their data gave

$$\int_{0.004}^{0.8} \frac{dx}{x}(F_2^{\mu p} - F_2^{\mu n}) = 0.227 \pm 0.007(\text{stat.}) \pm 0.014(\text{sys.})$$

at $Q^2 = 4$ GeV^2, as compared to the Gottfried sum

$$I_{\text{GSR}} = \int_0^1 \frac{dx}{x}(F_2^{\mu p} - F_2^{\mu n}) = \tfrac{1}{3}\int_0^1 dx(u_v - d_v) + \tfrac{2}{3}\int_0^1 dx(\bar{u} - \bar{d})$$

$$= \tfrac{1}{3} \qquad \text{if} \quad \bar{u} = \bar{d}. \tag{12}$$

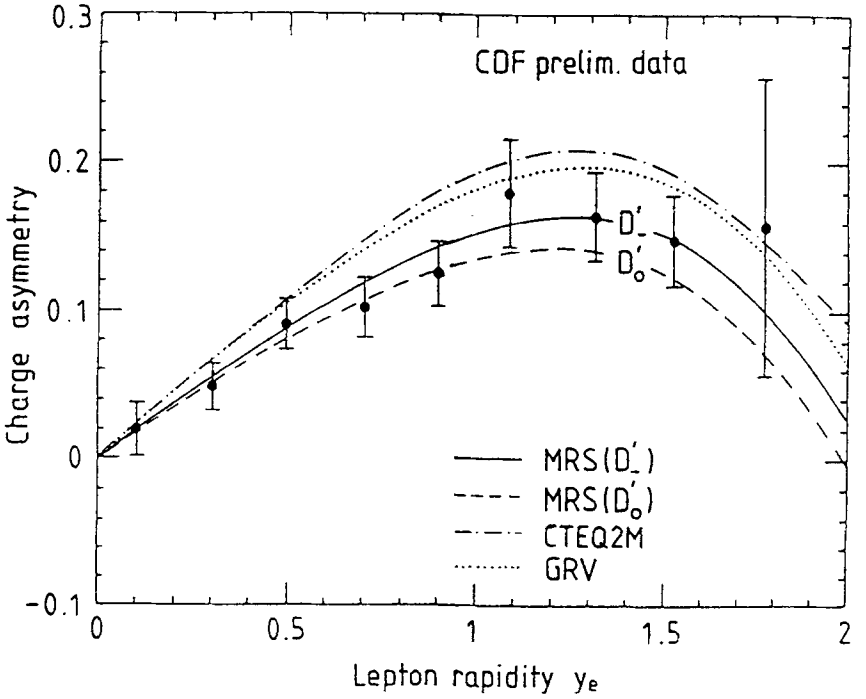

Figure 6. A plot of the CDF data for the lepton charge asymmetry, (11), compared to the predictions of various sets of partons [5, 18, 19]. The plot is taken from ref. [16]. These data were fitted in the MRS(A) analysis [20] which gives a description essentially equal to that of MRS(D'_).

Using their data to extrapolate over the unmeasured regions of x, NMC obtained $I_{\text{GSR}} = 0.240 \pm 0.016$ [21] [22]. The most plausible explanation of the difference between the NMC value and the Gottfried sum of $\frac{1}{3}$ is that $\bar{d} > \bar{u}$. In the MRS 'D' fits $\bar{d} - \bar{u}$ is parametrized according to (8) with the parameter A_Δ chosen to reproduce the measured value of I_{GSR}. It is interesting to note, however, that even including the NMC data, it is still possible to maintain $\bar{u} = \bar{d}$ and obtain an equally good global description of the data, but at the expense of a contrived small x behaviour of the valence distributions, as in set S'_0 of ref. [6]. The comparison of the $(F_2^p - F_2^n)$ NMC data with S'_0 and D'_0 is shown in Fig. 7 – the area under the curves gives $I_{\text{GSR}} = 0.333$ and 0.256 respectively, the difference coming primarily from the unmeasured $x \lesssim 10^{-2}$ region. The most physical assumption is to allow

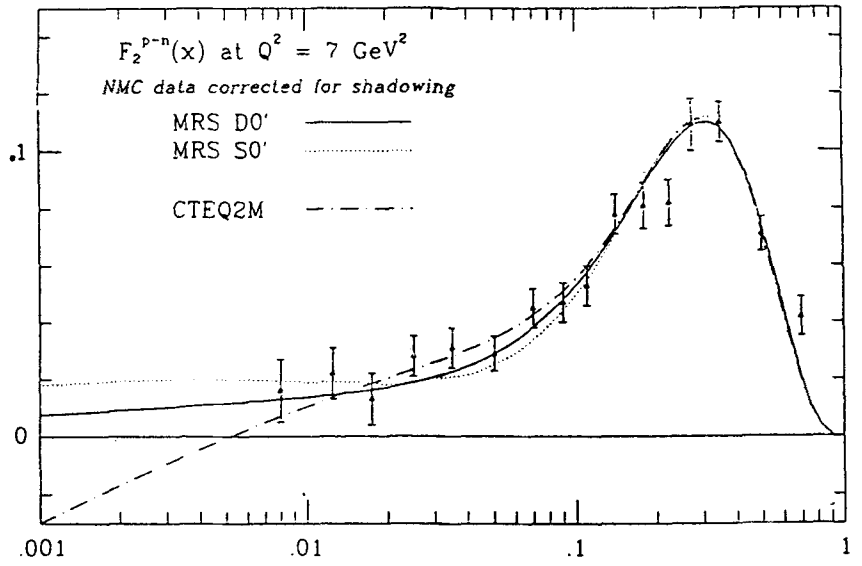

Figure 7. The structure function difference $F_2^{\mu p} - F_2^{\mu n}$ measured by NMC [22] compared with the description by partons from refs. [5, 18].

$\bar{u} \neq \bar{d}$, as in the 'D'-type fits. Nevertheless the conclusion is that the detailed structure of $\bar{d} - \bar{u}$ is not determined by the available deep-inelastic data.

As the $W^{\pm}$ rapidity asymmetry measurements improve they become increasingly sensitive to the behaviour of $\bar{u}$ and $\bar{d}$ in the region $x \simeq M_W^2/\sqrt{s}$. However a more direct method [24] to obtain information on $\bar{d} - \bar{u}$ is to compare (Drell-Yan) lepton-pair production in pp and pn collisions, via the asymmetry

$$A_{\rm DY} = \frac{\sigma_{pp} - \sigma_{pn}}{\sigma_{pp} + \sigma_{pn}}. \tag{13}$$

Because $u > d$ in the proton, the asymmetry $A_{\rm DY}$ is positive for parton sets with $\bar{d} - \bar{u}$ zero or small, but $A_{\rm DY}$ is reduced and can even be negative for parton sets with larger $\bar{d} - \bar{u}$ [25]. An asymmetry measurement by the NA51 collaboration [26],

$$A_{\rm DY} = -0.09 \pm 0.02 \pm 0.02 \tag{14}$$

at $x = 0.18$, was announced at this conference. This result, which implies $\bar{u}/\bar{d} \simeq 0.5$ at $x = 0.18$, corresponds to a breaking of flavour symmetry considerably beyond that associated with the MRS(D_0',D_-') partons and almost as large as that calculated using CTEQ2M partons, see Fig. 8.

We may conclude that, as far as the asymmetries are concerned, the MRS partons accurately reproduce the $W^{\pm}$ rapidity asymmetry (Fig. 6) but do not describe the new Drell-Yan asymmetry measurement. On the other hand the CTEQ partons describe the $W^{\pm}$ asymmetry rather poorly, but offer a much better description of the Drell-Yan asymmetry.

(d) Present status of parton distributions

We noticed that the high precision deep-inelastic data are well described by the parton distributions but that they do not pin down the $\bar{d} - \bar{u}$ combination. However

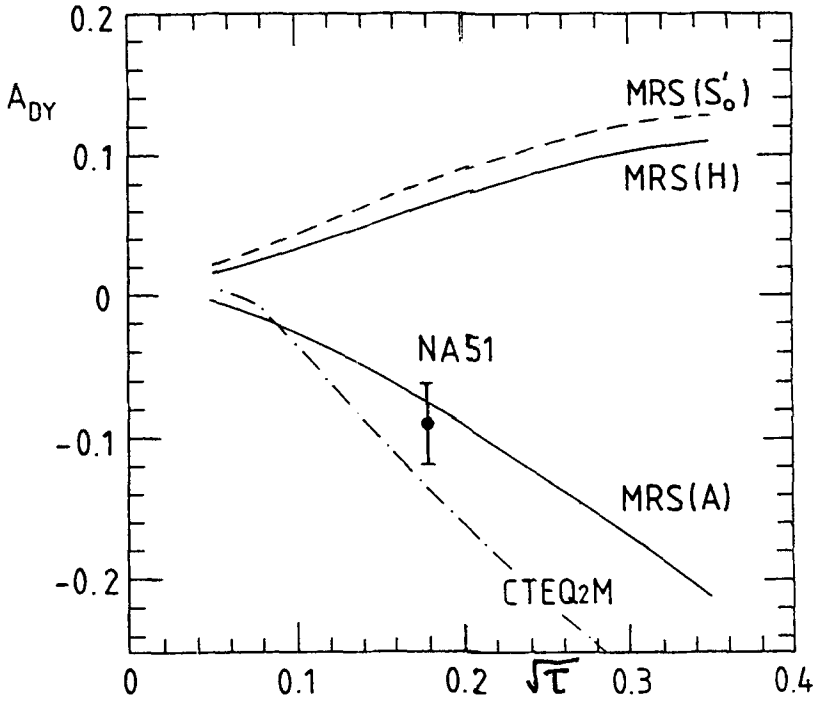

Figure 8. The *pp/pn* Drell-Yan asymmetry of (13) measured by NA51 [25] compared to values obtained by various sets of partons [5, 15, 20, 18]. The data point was included in the MRS(A) analysis [20].

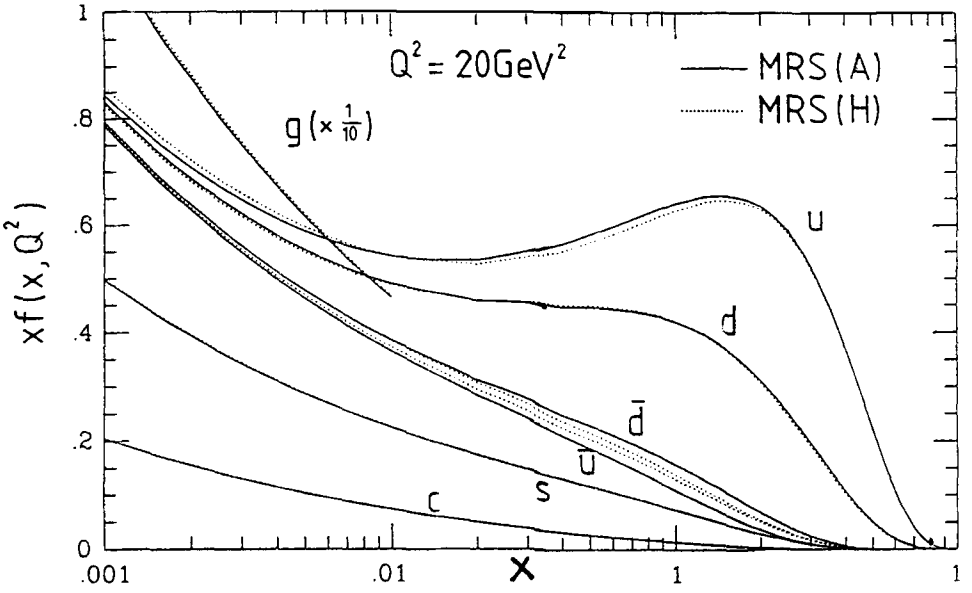

Figure 9. The MRS(A) [20] and MRS(H) [15] parton distributions at $Q^2 = 20$ GeV^2 shown by continuous and dotted curves respectively. Unlike MRS(H), MRS(A) incorporated constraints from the asymmetry data of Figs. 6 and 8 in the analysis.

other measurements give independent information on the partons. In particular the new asymmetry measurements probe fine details of the quark distributions.

Can we use the residual freedom of $\bar{d} - \bar{u}$ to modify the MRS(H) set of partons so as to describe the new Drell-Yan asymmetry measurement [26] while maintaining the quality of the global fit to the data? In particular can we maintain the quality of the description of the $W^{\pm}$ asymmetry (Fig. 6) and of the accurate NMC measurements of F_2^n/F_2^p? It turns out that such a fit is possible – we denote the new set of partons by MRS(A) [20]. The asymmetries resulting from this set of partons are shown in Figs. 6 and 8. We would expect the MRS(A) partons to be very similar to those of MRS(H), except that $\bar{d} - \bar{u}$ would be much larger while at the same time approximately conserving $\bar{u} + \bar{d}$, $d + \bar{d}$ and $u + \bar{u}$ (as required by (1)-(4)). Thus we anticipate an increase of $\bar{d}$ which is compensated by a corresponding decrease in $\bar{u}$ and d, which in turn requires a similar increase in u. The comparison of MRS(H) and MRS(A) parton sets is shown in Fig. 9, and displays these trends in the region $0.02 \lesssim x \lesssim 0.7$ where a full set of deep inelastic data exist.

Although the quark distributions are well-constrained by the data, the same is not so true for the gluon. Within the global analyses, we can identify three types of constraint on the gluon: (i) the momentum sum rule, (ii) the prompt photon production measurements and (iii) the observed overall pattern of scale violations, $\partial F_i/\partial \log Q^2$, for $x \lesssim 0.1$. The measurements of F_2^{ep} at HERA probe primarily the behaviour of the sea quark distributions at small x, although accurate measurements of $\partial F_2^{ep}/\partial \log Q^2$ will further constrain the gluon. If the observed steep rise of F_2 with decreasing x is attributed to the Lipatov or BFKL perturbative QCD mechanism via $g \to q\bar{q}$, then the same behaviour should be seen also in the gluon distribution. A direct measurement of the gluon in the $x \lesssim 10^{-2}$ region would be invaluable.

In addition to the potential constraints coming from accurate measurements of $\partial F_2/\partial \log Q^2$, there are several other possible ways of measuring the gluon at HERA, including F_L, J/ψ, $Q\bar{Q}$... production. In principle the observation of the longitudinal structure function is a gold-plated measurement, but in practice it will be difficult. To extract F_L as a function of x, Q^2, requires observation of the $y = Q^2/xs$ dependence of deep inelastic scattering, which means having electron-proton collisions at different c.m. energies $\sqrt{s}$.

There are also possibilities to obtain information on the gluon from hadron colliders, in particular the Fermilab $p\bar{p}$ collider. At $\sqrt{s} = 1.8$ TeV, x values comparable to those currently measured at HERA can be probed either by observing small mass systems produced centrally (e.g. $b\bar{b}$ or Drell-Yan production or by more massive final states at large rapidity y (e.g. same-side W+jet or dijet production). As an illustration Fig. 10 shows the ratio of same-side to opposite-side jet cross sections from uncorrected CDF data, as a function of the equal and opposite rapidities y. At large y the same-side cross section originates dominantly from subprocesses of g(small x)$q_{\rm val}$(large x) origin. The curves are the MRS(D$'_-$,D$'_0$,H) predictions evaluated at leading order with a renormalization/factorization scale chosen to mimic the next-to-leading order corrections. Further details of this analysis can be found in ref. [27]. We see that at large rapidity the ratio is sensitive to the small x behaviour of the gluon and that the preliminary CDF data favour the singular distributions. Dijet production from 'direct' photons at HERA offers similar possibilities of probing the gluon at small x via $\gamma g \to q\bar{q}$ [28].

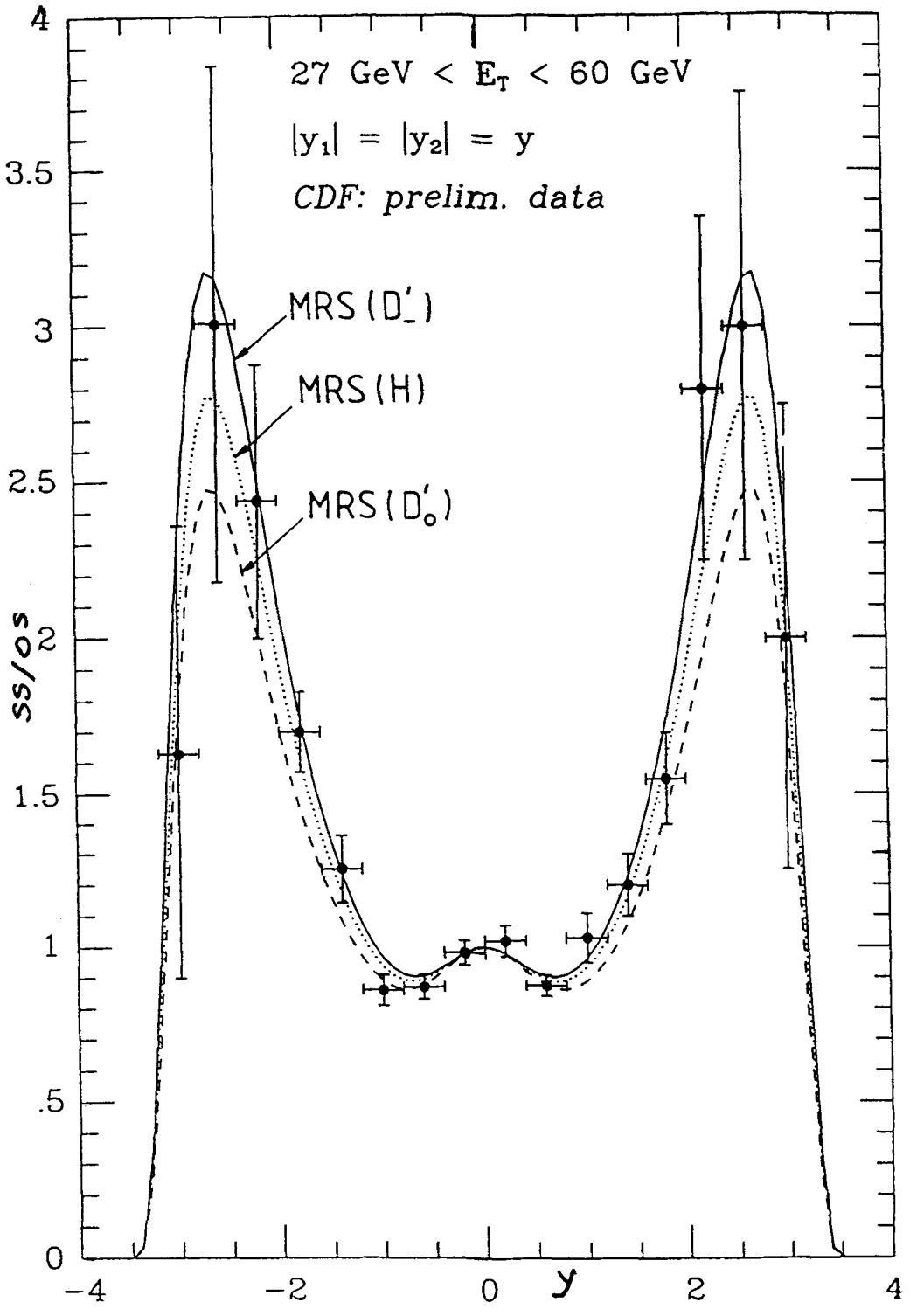

Figure 10. The same-side/opposite-side dijet ratio predicted by parton sets of refs. [5, 15] compared with preliminary, uncorrected CDF data.

3. Conclusions

The parton densities of the proton are well determined in the region $0.02 \lesssim x \lesssim 0.7$ where high precision data for a wide range of deep-inelastic and related processes are available. The one combination, $\bar{d} - \bar{u}$, that is not constrained by the deep-inelastic data, has for the first time been determined at $x = 0.18$ by a measurement of the Drell-Yan asymmetry in pp and pn collisions [26]. This measurement, together with the $W^{\pm}$ rapidity asymmetry measurements probe fine details of the quark densities. It is therefore not surprising that the existing MRS (and CTEQ) partons require minor modification. The result is a new set of partons [20] – MRS(A) – which is essentially identical to MRS(H) at small x; recall that the latter parton set [16] was obtained by incorporating the 1992 HERA measurements of F_2 [3, 4] into the analysis. It is found that MRS(A,H) also give an excellent description of the new preliminary 1993 higher statistics HERA data for F_2.

Acknowledgements

I thank Alan Martin and James Stirling with whom I collaborated on the MRS analysis presented here. I warmly thank Uma Sankar and DP Roy for inviting me to this excellent workshop.

References

[1] BCDMS collaboration: A.C. Benvenuti et al., Phys. Lett. B**223** (1989) 485

[2] NMC: P. Amaudruz et al., Phys. Lett. B**295** (1992) 159

[3] H1 collaboration: I. Abt et al., Nucl. Phys. B**407** (1993) 515

[4] ZEUS collaboration: M. Derrick et al., Phys. Lett. B**316** (1993) 412

[5] In principle s and $\bar{s}$ could be distinguished by accurate νN and $\bar{\nu} N$ data.

[6] A.D. Martin, R.G. Roberts and W.J. Stirling, Phys. Lett. B**306** (1993) 145

[7] E.A. Kuraev, L.N. Lipatov and V.S. Fadin, Sov. Phys. JETP **45** (1977) 199
Ya.Ya. Balitsky and L.N. Lipatov, Sov. J. Nucl. Phys. **28** (1978) 822

[8] CCFR collaboration: A. Bazarko et al., Columbia University preprint NEVIS-1492 (1993)

[9] V. Barone et al., Phys. Lett. B**268** (1991) 279

[10] NMC: P. Amaudruz et al., Phys. Rev. Lett. **66** (1991) 2712

[11] A.D. Martin, R.G. Roberts and W.J. Stirling, Phys. Lett. B**228** (1989) 149

[12] W.-K. Tung, these proceedings
S. Brodsky, contribution to this workshop

[13] V.N. Gribov and L.N. Lipatov, Sov. J. Nucl. Phys. **15** (1972) 438
G. Altarelli and G. Parisi, Nucl. Phys. B**126** (1977) 298
Yu.L. Dokshitzer, Sov. Phys. JETP **46** (1977) 641

[14] M. Virchaux and A. Milsztajn, Phys. Lett. B**272** (1992) 221

[15] CCFR collaboration: S.R. Mishra, Proc. of Lepton-Photon Symposium, Geneva (1991); P.Z. Quintas et al., Phys. Rev. Lett. **71** (1993) 1307

[16] A.D. Martin, R.G. Roberts and W.J. Stirling, Proc. Workshop on Quantum Field Theoretical Aspects of HE Physics, Kyffhäusser, Germany, eds. B. Geyer and E.-M. Ilgenfritz, Leipzig (1993) p. 11

[17] A.D. Martin, R.G. Roberts and W.J. Stirling, Mod. Phys. Lett. **A4** (1989) 1135
E.L. Berger, F. Halzen, C.S. Kim and S. Willenbrock, Phys. Rev. **D40** (1989) 83, E3789

[18] CTEQ collaboration: J. Botts et al., Phys. Lett. **B304** (1993) 159, now superseded by CTEQ2.

[19] M. Glück, E. Reya and A. Vogt, Z. Phys. **C53** (1992) 127; Phys. Lett. **B306** (1993) 391

[20] A.D. Martin, R.G. Roberts and W.J. Stirling, preprint RAL-94-055, DTP/94/34., to appear in Phys. Rev.

[21] NMC: M. Arneodo et al., CERN preprint PPE/93-117 (1993)

[22] An updated analysis of the Gottfried sum by NMC [21] gives $I_{\rm GSR} = 0.258 \pm 0.010$ (stat.) ± 0.015 (sys.) at $Q^2 = 4$ GeV^2. If $F_2^{\mu n}$ is corrected for deuteron screening effects then $I_{\rm GSR}$ is reduced to $\simeq 0.23$.

[23] NMC: E.M. Kabuss, Nucl. Phys. B (Proc. Suppl.) **29A** (1992) 1

[24] S.D. Ellis and W.J. Stirling, Phys. Lett. **B256** (1991) 258

[25] A.D. Martin, R.G. Roberts and W.J. Stirling, Phys. Lett. **B308** (1993) 377

[26] NA51 collaboration: A. Baldit et al., Phys. Lett. to be published.

[27] A.D. Martin, R.G. Roberts and W.J. Stirling, Phys. Lett. **B318** (1993) 184

[28] J.R. Forshaw and R.G. Roberts, Phys. Lett. **B319** (1993) 539; RAL preprint-94-028 (1994)